

Interfacing sequential injection on-line preconcentration using a renewable micro-column incorporated in a 'lab-on-valve' system with direct injection nebulization inductively coupled plasma mass spectrometry

Jianhua Wang and Elo Harald Hansen*

Department of Chemistry, Technical University of Denmark, Building 207, Kemitorvet, DK-2800 Kgs. Lyngby, Denmark. E-mail: ehh@kemi.dtu.dk

Received 25th June 2001, Accepted 24th September 2001

First published as an Advance Article on the web 14th November 2001

A sequential injection (SI) on-line 'lab-on-valve' separation/preconcentration system incorporating a renewable ion-exchange micro-column interfaced with inductively coupled plasma mass spectrometry (ICP-MS) via a home-made direct injection high efficiency nebulizer (DIHEN) is described. Aimed at eliminating spectroscopic and non-spectroscopic interferences, the renewable micro-column is first loaded by aspirating 15 μl of a SP Sephadex C-25 cation-exchanger bead suspension and then exposed to a defined volume of sample solution. Residuals of matrix components are pre-eluted with carrier solution (nitric acid, 1 : 80 v/v), and the measurands are subsequently eluted with a defined volume of nitric acid (1 : 16 v/v). The leading volume of eluate (ca. 30 μl) is collected and introduced into the plasma via the DIHEN. The eluted beads are then discarded and a new column is aspirated for the next operation. Data acquisition is performed in parallel with the ensuing preconcentration process. With 2.0 ml sample loading, the enrichment factors are 35.2 (0.05–2.4 $\mu\text{g l}^{-1}$) for Ni, and 9.1 (0.04–1.6 $\mu\text{g l}^{-1}$) and 28.4 (1.6–3.2 $\mu\text{g l}^{-1}$) for Bi. The detection limits (3σ) are 15 ng l^{-1} (Ni) and 4 ng l^{-1} (Bi), while the sampling frequency is 12 per hour. The precisions are 2.9% (0.8 $\mu\text{g l}^{-1}$ Ni) and 1.7% (0.8 $\mu\text{g l}^{-1}$ Bi). The procedure is validated by determination of nickel and bismuth in a certified reference material (CRM 320, River Sediment), and the recoveries are measured by spiking two human urine samples.

Introduction

Inductively coupled plasma mass spectrometry (ICP-MS) is one of the most powerful techniques for trace multi-element measurements. Interferences due to both spectroscopic and non-spectroscopic effects do, however, make its application somewhat complicated.¹

Some reduction of spectral interferences can be obtained by using a cold plasma,² a shielded torch,³ a mixed gas plasma,⁴ or a collision cell,⁵ but the applications are restricted. Sector field ICP-MS can effectively eliminate spectral interferences,⁶ but it is very costly and, with regard to matrix effects, it does not compare well with quadrupole ICP-MS.⁷ Arithmetic correction is useful only if contributions from polyatomic ions are limited,^{8,9} which in many cases does not hold true.¹

Non-spectral interferences due to matrix effects can be reduced by sample dilution,¹⁰ but this results in an undesired high limit of quantification which might be further degraded by spectral interferences. Internal standardization^{11,12} is only practical if the standard and measurand are closely matched in both mass and ionization energy.^{1,13} Standard addition is useful in many cases,¹ although it is time consuming. Matrix matching can be used in specific cases,^{1,14} provided that there is sufficient information about the constitution of the matrix.

The most effective way to eliminate or attenuate non-spectral and spectral interferences arising from the matrix is simply to isolate the measurand from the matrix. This can conveniently and effectively be done by applying appropriate flow injection/sequential injection (FI/SI) on-line separation/preconcentration schemes. In addition to reducing sample/reagent consumption and sample preparation time, the risks of sample contamination from the environment are minimized.

Various procedures for FI on-line separation/preconcentration with detection by ICP-MS have been described, including hydride generation,^{15,16} ion-exchange,^{17,18} adsorption and (co)precipitation.^{19–21} Ion-exchange is one of the simplest and most effective methods. It has been pointed out,^{22–24} however, that many sorbent materials contained within a column reactor are prone to build-up of back pressure caused by progressively tighter packing. Additionally, their surface properties, associated with loading and elution kinetics, might be irreversibly changed due to contamination, deactivation or even loss of functional groups. In order to overcome these drawbacks, a novel approach for on-line ion-exchange sample pretreatment, using a renewable micro-column, based on sequential bead injection in a 'lab-on-valve' system applied in conjunction with detection by ETAAS was recently described.^{22,23} In the system a micro-column was packed by aspirating a well-defined quantity of ion-exchange resin beads into a channel cavity of the 'lab-on-valve', followed immediately by sample loading. The loaded beads were afterwards either transported directly into the graphite tube for quantification,²² or eluted by a metered volume of eluent. This volume of eluant, sandwiched by two air segments, was transferred into the detector, whereupon the beads were discarded.²³

The latter approach appears to be adaptable for ICP-MS, although the interface between the FI/SI system and the plasma requires modifications, because air must be excluded in order to protect the plasma (and the use of argon segmentation would make the system unnecessarily complicated). In this paper the design of a sequential injection 'lab-on-valve' preconcentration system with a renewable micro-column successfully interfaced with ICP-MS is described. Since the volume of eluate obtained after the on-line separation and preconcentration is limited

Table 1 Operating conditions for the ICP-MS detection system

<i>ICP-MS</i>	
RF power/kW	1.2
Sampling depth/mm	10
Sampling cone (orifice mm ⁻¹)	Pt (1.1)
Skimmer cone (orifice mm ⁻¹)	Pt (0.9)
Plasma gas flow/l min ⁻¹	12
Auxiliary gas flow/l min ⁻¹	1.2
Bessel box barrel (B)	47 (digipots)
Bessel box plate lens (P)	45
Photo stop lens (S2)	47
Einzel lenses (E1)	23
<i>DIHEN</i>	
Capillary id/ μ m	75
Capillary od/ μ m	176
Gas annulus area/mm ²	0.0071
Sample flow rate/ μ l min ⁻¹	60
Nebulizer gas flow/l min ⁻¹	0.23
Back pressure/psi ^a g	43
<i>Data acquisition</i>	
Scanning mode	Peak hopping
Dwell time/ms	50
Sweeps per reading	25
Readings per replicate	1
Replicates	3
^a 1 psi \approx 6894.757 Pa.	

(ca. 30 μ l), the use of a micro-flow high efficiency nebulizer is required. Many micro-flow nebulizers have so far been introduced, including the high efficiency nebulizer (HEN),²⁵ the micro-concentric nebulizer (MCN),²⁶ the direct injection nebulizer (DIN),²⁷ the direct injection high efficiency nebulizer (DIHEN)²⁸ and the micro-flow ultrasonic nebulizer (μ -USN).²⁹ In particular the nebulizers with 100% sample transport efficiency, that is, the DIN and the DIHEN, have attracted much attention. The application of the DIN is, however, restricted by its high costs and the need of a high-pressure gas displacement pump for sample delivery as well as an auxiliary nebulizer gas. A DIHEN design was therefore adopted and developed for use with the specific sequential bead injection system.

The practical applicability of the procedure is tested by assays of nickel and bismuth in biological and environmental samples.

Experimental

Reagents and samples

All reagents used were at least of analytical-reagent grade.

Milli-Q water (18.2 M Ω cm) was used throughout. Suprapur nitric acid (Merck) was further purified by sub-boiling distillation. Working standard solutions were obtained by step-wise dilution of 1000 mg l⁻¹ standard solutions of nickel

(Merck) and bismuth (Perkin-Elmer) with a 0.10 M potassium acetate buffer of pH 4.2. The cation-exchange resin, SP Sephadex[®] C-25 (Pharmacia Biotech AB, dry bead size 40–125 μ m), was converted to the K⁺ and H⁺ forms²² and suspended in Milli-Q water (1 : 10–1 : 20 w/v).

Other chemicals used were: HClO₄ (70%, Merck), HF (40%, Merck), acetic acid glacial (100%, Merck) and potassium acetate (BDH).

Community Bureau of Reference (BCR) CRM-320 River Sediment. 0.1 g of CRM 320 was weighed out and transferred to a PTFE beaker to which 3.0 ml of concentrated nitric acid and 2.5 ml of 40% HF were added. The sample was soaked for 1 h, and then heated gently on a sand bath until fumes appeared and the solution had nearly dried. After cooling, 1.0 ml of concentrated perchloric acid was added, and the contents were heated to near dryness again. The contents were dissolved with 3.0 ml nitric acid (1 : 16 v/v), transferred to a polyethylene flask and diluted to 100 ml with 0.10 M acetate buffer (pH 4.2).

Urine samples. 10 ml of urine were transferred into a PTFE beaker, and 10 ml of concentrated nitric acid were added. The mixture was heated gently on a sand bath to near dryness. After cooling, 1.0 ml of concentrated perchloric acid was added and the solution was heated to near dryness again. The contents were dissolved with 3.0 ml nitric acid (1 : 16 v/v), transferred to a polyethylene flask and diluted to 100 ml with 0.1 M acetate buffer (pH 4.2).

Spiking of urine samples was carried out by adding 40 μ l of a solution containing 1000 μ g l⁻¹ of Ni and Bi, respectively, to 10 ml of urine. The spiked solutions were allowed to stand overnight for equilibration.

Instrumentation and procedure

An Elan 5000 ICP-MS system (Perkin-Elmer SCIEX, Concord Ontario, Canada) was used, the operating parameters being summarized in Table 1.

A schematic diagram of the direct injection high efficiency nebulizer (DIHEN) is shown in Fig. 1. A PEEK adapter (home-made) was mounted with a borosilicate glass tube (id 2.9 mm, od 6.0 mm, length 176 mm) with a 0.2 mm orifice in the tapered nozzle. A fused silica capillary (Polymicro Technologies, id 75 μ m, od 200 μ m, 12 μ m coating) was used as the sample capillary, resulting in a gas annulus area of 0.0071 mm² (the coating in the tip was removed). The capillary was supported by PEEK tubing (id 254 μ m, od 1.6 mm, Upchurch) that extended to 55 mm below the nebulizer tip. A piece of Tygon tubing (id 190 μ m, od 2.1 mm, length 5 mm) was inserted into the tapered end of the PEEK tubing to prevent the nebulizer gas from flowing back. A copper coil was used to hold the PEEK tubing in the middle of the glass tube. The dead volume of the DIHEN is approximately 1.2 μ l.

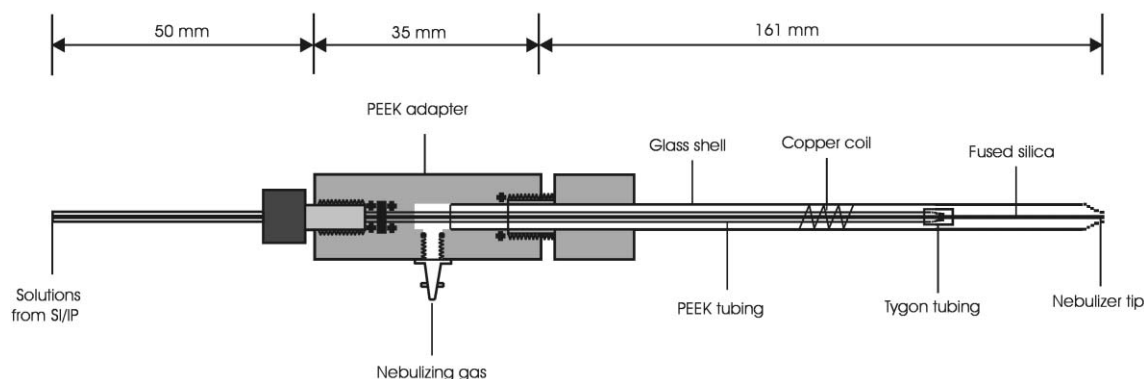


Fig. 1 Schematic diagram of the direct injection high efficiency nebulizer (not scaled).

The DIHEN was interfaced with the ICP-MS instrument by inserting it into the torch adapter, with the tip positioned approximately 2 mm below the intermediate tube of the torch. A well-shaped fine aerosol that was confined right in the center of the torch was obtained when the capillary tip exceeded the nozzle surface by *ca.* 0.2 mm. In contrast to the DIN,²⁷ neither a high pressure pump nor an auxiliary nebulizer gas is necessary. A test of robustness showed that no visible deformation or damage to the nebulizer tip was observed after 120 h of operation under the conditions applied.

The flow rate of the external nebulizer gas supply for the DIHEN was controlled by a mass flow controller (Zimser Proces-Instrumentering Aps, Denmark).

The automated on-line separation/preconcentration system was a FIALab-3500 FIA/SIA system (FIALab, USA), equipped

with a 6-port selection valve (SV) mounted with an integrated 'lab-on-valve' micro-system. Furthermore, a syringe pump (SP, 2.5 ml) and an auxiliary peristaltic pump were used.

The SI-manifold and the integrated micro-conduit of the 'lab-on-valve' system are shown in Fig. 2. Of the 7 micro-channels (id 1.66 mm, length 12.0 mm), two (communicating with port 4 and the central port) served as micro-columns for accommodating the ion-exchange beads. A small piece of PEEK tubing (id 17.8 μm , length 3.5 mm) was inserted into these two channels in order to hold the beads within them and prevent the beads from escaping. Details and other characteristics of the 'lab-on-valve' system have been described previously.²²

An infusion pump (kdS 101, KD Scientific, USA) was used for carrier/sample delivery into the ICP. A glass-wool filter

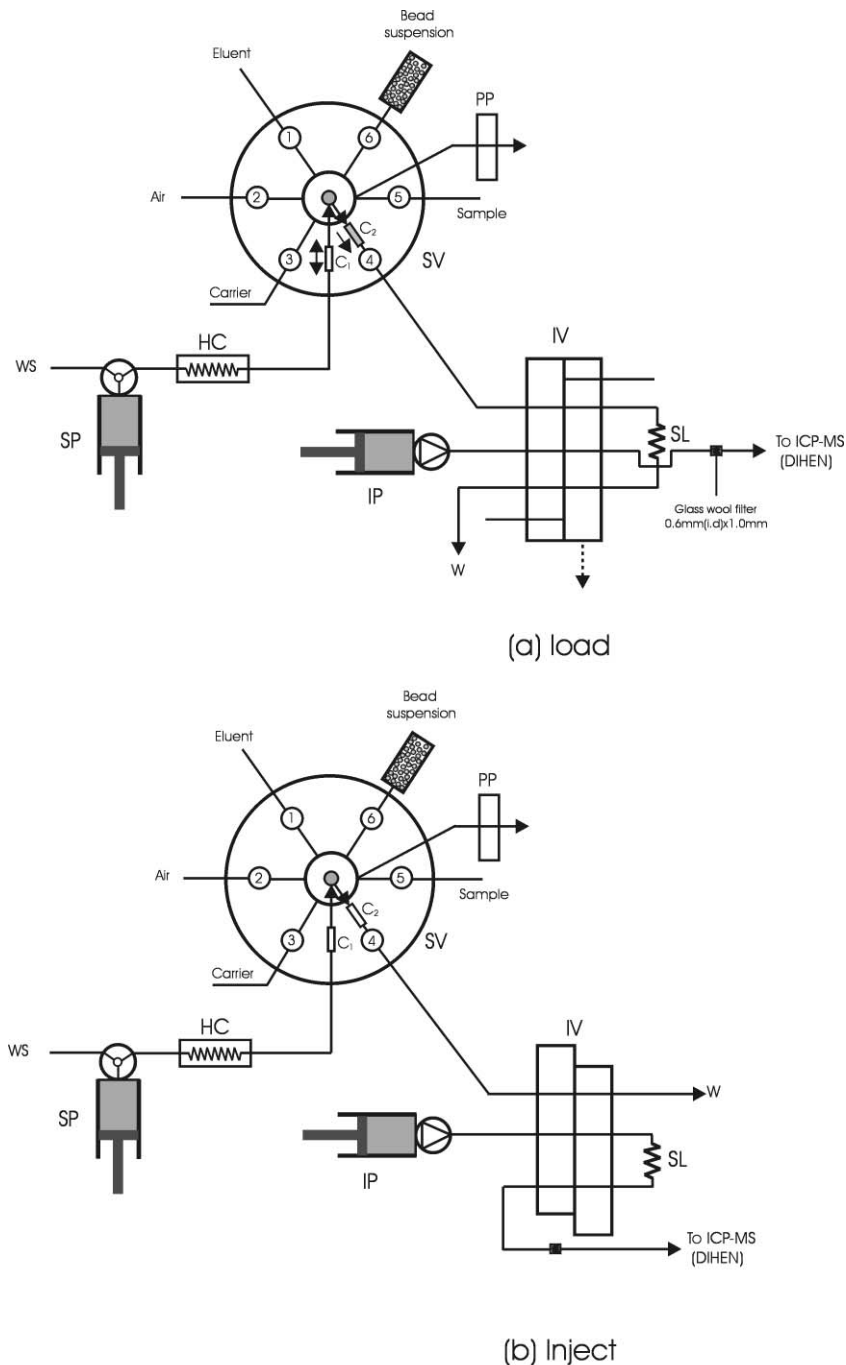


Fig. 2 Manifold for the sequential bead injection, on-line preconcentration: SV, 6-port selection valve; SP, syringe pump; IP, infusion pump; IV, injection valve; SL, sample loop; PP, peristaltic pump; HC, holding coil; and C₁, C₂, micro-columns (directions indicated). (a) Load position and (b) inject position.

(id 0.6 mm, length 1.0 mm), housed in a piece of PTFE tubing (id 0.6 mm, od 1.6 mm), was introduced between the sample loop and the DIHEN in order to prevent escaped beads from reaching the DIHEN and blocking the capillary.

All externally used tubes were made from PTFE of id 0.50 mm, except for the line from the infusion pump to the nebulizer that had an id of 0.30 mm (od 1.6 mm).

The operating procedure for the SI-system (Fig. 2) has the following protocol. The bead suspension is first aspirated into and settled in the lower part of a 1.0 ml plastic syringe, which is mounted in port 6. Port 5 is connected to both the sample solution and the peristaltic pump. On changing the sample, the pump is started in order to aspirate the sample solution past the central flow-through port, whereupon it is stopped.

A separation and preconcentration cycle runs through 4 steps. The injection valve (IV) is switched to the *load* position [Fig. 2(a)] before starting the operation. The carrier stream (1 : 80 v/v nitric acid) is pumped continuously into the ICP by the infusion pump (IP).

Step 1: Preconditioning. 600 µl of carrier solution are aspirated into the holding coil (HC) at a flow rate of $150 \mu\text{l s}^{-1}$; 480 µl of the carrier are subsequently directed to port 4 ($100 \mu\text{l s}^{-1}$) to rinse column C_2 , thus leaving 120 µl in the holding coil.

Step 2: Preconcentration. 2.0 ml of sample solution are aspirated ($150 \mu\text{l s}^{-1}$) into the HC and 15 µl of bead suspension are slowly ($3 \mu\text{l s}^{-1}$) aspirated into C_1 . Thereafter, the beads are transported to column C_2 through port 4 ($12 \mu\text{l s}^{-1}$) along with the sample solution, that is, the preconcentration process is taking place. The 120 µl carrier from step 1 is used to wash/ 'pre-elute' the column (see section on Interferences below). 500 µl of carrier ($100 \mu\text{l s}^{-1}$) and 360 µl of air ($60 \mu\text{l s}^{-1}$) are aspirated afterwards. 160 µl of air are propelled through port 4 ($25 \mu\text{l s}^{-1}$), thereby leaving the line from the central port to the sample loop (SL) filled with air.

Step 3: Elution. 60 µl of nitric acid (1 : 16 v/v) are aspirated into C_1 ($5 \mu\text{l s}^{-1}$). The central port is then directed to port 4, valve IV is switched to the *inject* position [Fig. 2(b)], the SP is moved forward ($12 \mu\text{l s}^{-1}$), whereby micro-column C_2 is eluted, and the leading part of the eluate is stored in the sample loop, SL, as identified *via* the expulsion of the air previously stored in the communicating line. Afterwards, valve IV is switched back to the *load* position, and the eluate is introduced into the ICP *via* the DIHEN. Data acquisition is initiated 25 s after IV is switched back.

Step 4: Discarding the used beads. With the central port connected to port 4, SP is moved forward to propel the carrier solution at a higher flow rate ($100 \mu\text{l s}^{-1}$). Thereby the beads become squeezed and pass through the narrow exit in column C_2 ,²³ that is, all the resin beads are flushed out and discarded.

Results and discussion

Selection of monitored isotopes

The ^{58}Fe isobaric overlap excludes the use of the most abundant isotope of Ni, *i.e.*, ^{58}Ni . Although the abundance of ^{58}Fe is low (0.28%), the iron content in biological and environmental samples might be 2 or 3 orders of magnitude higher than nickel.¹⁰ In addition, this isotope also tends to suffer interferences from some polyatomic ions.³⁰

^{61}Ni , ^{62}Ni and ^{64}Ni are not preferred because of their very low abundances. ^{62}Ni is sometimes chosen,¹⁷ but it suffers serious interference from $^{23}\text{Na}^{23}\text{Na}^{16}\text{O}$ in biological samples.⁸ The present authors previously demonstrated that ^{60}Ni is most suitable for the determination of nickel in biological samples by

ICP-MS;¹⁰ the potential interfering polyatomic ions include $^{44}\text{Ca}^{16}\text{O}$, $^{43}\text{Ca}^{16}\text{O}^{1}\text{H}$, $^{42}\text{Ca}^{18}\text{O}$, $^{37}\text{Cl}^{23}\text{Na}$, $^{35}\text{Cl}^{25}\text{Mg}$ and $^{36}\text{Ar}^{24}\text{Mg}$. The effect of $^{42}\text{Ca}^{18}\text{O}$ and $^{43}\text{Ca}^{16}\text{O}^{1}\text{H}$ cause no trouble because of the low abundance of ^{42}Ca , ^{43}Ca and ^{18}O , and the formation of $^{43}\text{Ca}^{16}\text{O}^{1}\text{H}$ causes less interference as compared with the diatomic ions. The formation of chloride-containing polyatomic ions is avoided due to the cation-exchange separation. The present studies also indicate that only a small part of Ca^{2+} and Mg^{2+} are retained by the beads, the majority of which can be eliminated by a pre-elution step (see Interferences section below). The effects of $^{44}\text{Ca}^{16}\text{O}$ and $^{36}\text{Ar}^{24}\text{Mg}$ are, therefore, minimized.

Bismuth is monatomic (^{209}Bi) and there is no isobaric overlap. One possible spectral interference could arise from $^{193}\text{Ir}^{16}\text{O}$ (ref. 31), which might be a problem in geological samples, but Ir is hardly present in biological and general environmental samples. Therefore, effort was focused on elimination of the matrix effect for bismuth, which is expected to be achieved following the on-line separation/preconcentration process.

Instead of using internal standards, a calibration standard of $0.4 \mu\text{g l}^{-1}$ was analysed periodically (2 h period) to ensure that the instrument response drift was acceptable, *i.e.*, $\pm 10\%$. At this level the drift over a 6 h period was found to be within the required range.

Optimization of ICP-MS operating parameters

Optimization was effected by the univariate approach. The effects of rf power, nebulizer gas flow rate and sample uptake flow rate are shown in Figs. 3–5. It is apparent from Fig. 3 that the signal intensity for nickel increased with increasing rf power, while the intensity of bismuth remained almost constant within the range of 1.0–1.2 kW, and afterwards decreased with increasing rf power. The results for bismuth are different from those reported by McLean *et al.*²⁸ for their DIHEN, where the signal intensities for the elements across the mass range kept increasing from 0.9 to 1.6 kW. Unfortunately, no specific data for bismuth were reported by these authors. By compromising between the sensitivities of nickel and bismuth, an rf power of 1.2 kW was selected for the present experimental series.

From Fig. 4 it can be seen that low nebulizer gas flow rates, within a rather narrow range, are preferred for the DIHEN. The sensitivities of both nickel and bismuth dropped rapidly as the nebulizer gas flow rate increased above 0.3 l min^{-1} , while the plasma became unstable at very low nebulizer gas flow rates (near 0.17 l min^{-1}). This might be attributed to the fact that, at low flow rates, relatively large droplets are formed in the

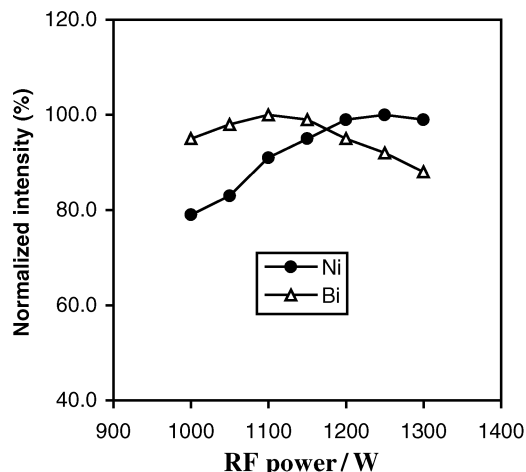


Fig. 3 The effect of the rf power as obtained under the following conditions: $10.0 \mu\text{g l}^{-1}$ (Ni^{2+} , Bi^{3+}); uptake flow rate, $40 \mu\text{l min}^{-1}$; and nebulizer gas flow rate, 0.23 l min^{-1} .

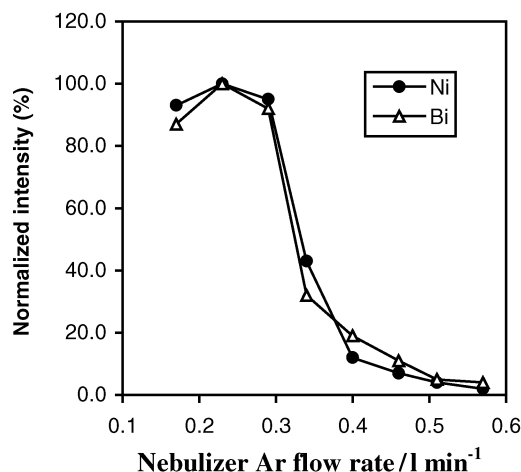


Fig. 4 The effect of the nebulizer gas flow rate as obtained under the following conditions: $10.0 \mu\text{g l}^{-1}$ (Ni^{2+} , Bi^{3+}); uptake flow rate, $40 \mu\text{l min}^{-1}$; and rf power, 1.2 kW.

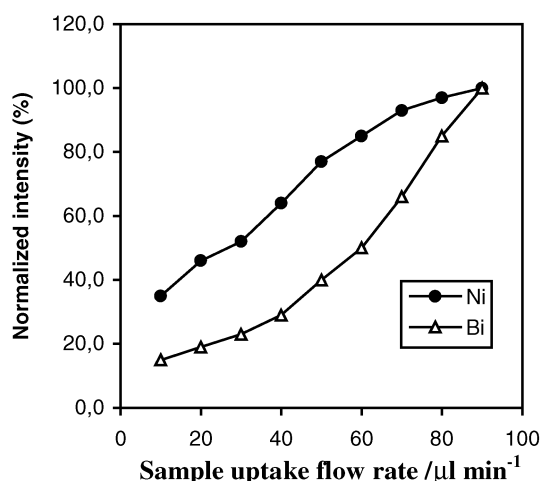


Fig. 5 The effect of uptake flow rate as recorded under the following conditions: $10.0 \mu\text{g l}^{-1}$ (Ni^{2+} , Bi^{3+}); nebulizer gas flow rate, 0.23 l min^{-1} ; and rf power, 1.2 kW.

aerosol (flicker was virtually observable from the nebulizer tip). For the ensuing experiments, the nebulizer gas flow rate was fixed at 0.23 l min^{-1} .

Fig. 5 shows that the signal intensities increased substantially with increasing sample uptake flow rates within the range of $10 \mu\text{l min}^{-1}$ to $80 \mu\text{l min}^{-1}$ (the highest flow rate tested). At the same time the detection limits were also improved (see Table 2).

As the sensitivities for both nickel and bismuth were sufficiently high, a sample uptake flow rate of $60 \mu\text{l min}^{-1}$ was chosen throughout. In fact, a further increase of the flow rate might cause higher back pressure in the capillary of the DIHEN. Additionally, excessive loading of solutions into the plasma should be avoided.

The experiments also showed that the signals of both nickel and bismuth returned to the blank level within 80 s from the appearance of the peaks. This coincided with the next sample being processed in the 'lab-on-valve' system, and no further wash-out procedure was necessary.

Under the above-mentioned conditions, the eluted band yielded a transient peak width at half peak maximum of approximately 30 s, which is sufficient for data acquisition.

Optimization of chemical variables

The effects of acidity, form of the ion-exchanger, eluent concentration and its corresponding volume were studied using both ICP-MS and ETAAS detection. The results showed that, for the beads on the K^+ - and H^+ -form of the resin, the enrichment efficiencies were at the same level for both nickel and bismuth within the pH range 3.4–5.2 (Ni) and 3.0–4.8 (Bi). The blanks, however, were higher for the K^+ -form than for the H^+ -form, which led to higher detection limits. The beads on the H^+ -form were therefore used. An acidity of pH 4.2, at which reasonable sensitivities for both nickel and bismuth could be achieved, was chosen. As to the eluent, nitric acid is a prerequisite for detection by ICP-MS. The results indicated that the retained nickel and bismuth were not eluted by nitric acid of less than 1.25% (v/v), while the majority of the ions (>90%) were eluted with $30 \mu\text{l}$ of nitric acid of 6.25% (v/v). $60 \mu\text{l}$ of nitric acid (6.25%) was thus aspirated into the 'lab-on-valve' system for elution, and the leading part of the eluate (ca. $30 \mu\text{l}$) was directed into the sample loop (SL) and afterwards introduced into the ICP via the DIHEN. The extra amount of eluent was used in order to avoid introducing air into the sample loop, which might extinguish the plasma.

Optimization of SI variables

The experiments showed that, within the concentration range of 0.05 – $2.4 \mu\text{g l}^{-1}$ Ni and 0.04 – $3.2 \mu\text{g l}^{-1}$ Bi, the sensitivities increased linearly with increasing sample loading time and no evidence of break-through was observed up to 2.4 ml of sample (the largest volume tested, as the capacity of the syringe pump is 2.5 ml). As a compromise between the sampling frequency and the preconcentration efficiency, 2.0 ml of sample was introduced, corresponding to a loading time of 167 s.

It is critical to control the sample flow rate within a certain range in order to optimize the preconcentration process. The experimental results indicated that, within the range 4 – $12 \mu\text{l s}^{-1}$, the sensitivity for bismuth increased with increasing

Table 2 Characteristic performance for the SI-bead injection on-line ion-exchange preconcentration procedure for nickel and bismuth

	Bismuth		Nickel
Linear calibration range	0.04 – $1.6 \mu\text{g l}^{-1}$		0.05 – $2.4 \mu\text{g l}^{-1}$
Regression equations	$I = 10286C_{\text{Bi}} - 307.6$		$I = 13552C_{\text{Ni}} - 215.5$
Correlation coefficient	$r = 0.9992$		$r = 0.9975$
Enrichment factors ^a ($60 \mu\text{l s}^{-1}$)	9.1		35.2
Enrichment factors ^a ($80 \mu\text{l s}^{-1}$)	9.5		34.3
Sampling frequency	12 h^{-1}		12 h^{-1}
Detection limits ($n = 9$, $60 \mu\text{l s}^{-1}$)	4 ng l^{-1}		15 ng l^{-1}
Detection limits ($n = 9$, $80 \mu\text{l s}^{-1}$)	2 ng l^{-1}		13 ng l^{-1}
Precision (RSD, $n = 6$)	1.7% ($0.8 \mu\text{g l}^{-1}$)		2.9% ($0.8 \mu\text{g l}^{-1}$)
Sample consumption	2.0 ml		2.0 ml
Bead consumption	15 μl		15 μl

^aThe enrichment factors were obtained by comparing with direct introduction of sample solutions, which are all matrix matched, into the plasma via DIHEN.

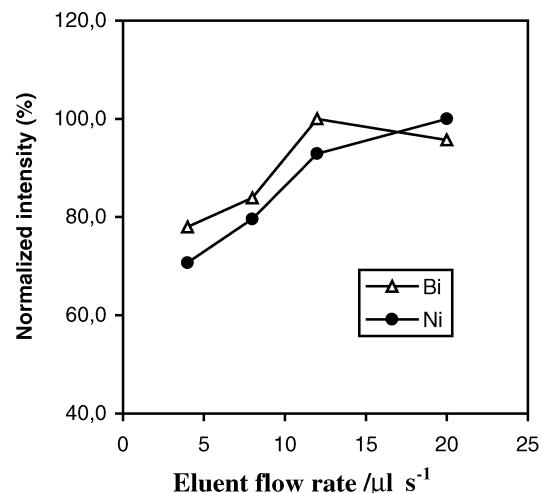


Fig. 6 The effect of the eluent (nitric acid) flow rate as obtained under the following conditions: $1.6 \mu\text{g l}^{-1}$ (Ni^{2+} , Bi^{3+}); nebulizer gas flow rate, 0.23 l min^{-1} ; nebulizer uptake flow rate, $40 \mu\text{ l min}^{-1}$; rf power, 1.2 kW ; sample flow rate, $12 \mu\text{ l s}^{-1}$; buffer pH 4.2 ; and sample loading time, 167 s .

flow rate, while it remained virtually unchanged for nickel. However, at sample flow rates above $15 \mu\text{ l s}^{-1}$, the sensitivities for both nickel and bismuth decreased and a rapid drop was observed at flow rates exceeding $30 \mu\text{ l s}^{-1}$, which can be attributed to the loss of beads.²³ A sample flow rate of $12 \mu\text{ l s}^{-1}$ was therefore chosen.

The effect of eluent flow rate is shown in Fig. 6. It is evident that the sensitivity of bismuth increased with increasing eluent flow rate and reached a maximum at a flow rate of $12 \mu\text{ l s}^{-1}$ followed by a decline, while the sensitivity of nickel kept increasing up to $20 \mu\text{ l s}^{-1}$. A flow rate of $12 \mu\text{ l s}^{-1}$ was thus adopted.

Interferences

The effects of some transition, alkaline earth and alkali metals on the preconcentration processes of nickel and bismuth using the Sephadex C-25 cation-exchange resin have been studied previously with detection by ETAAS.^{23,32} The conclusions drawn then hold true in the present experiments, *i.e.*, for most biological and environmental samples (digests), the contents of Cu^{2+} , Fe^{3+} , Pb^{2+} , Mn^{2+} , Co^{2+} , Cd^{2+} , Zn^{2+} and alkaline earth metals do not exceed the tolerance limits. The effects of Ca^{2+} and Mg^{2+} , however, were further investigated at this juncture, using both ICP-MS and ETAAS detection, because of the potential interferences of $^{44}\text{Ca}^{16}\text{O}$ and $^{36}\text{Ar}^{24}\text{Mg}$ on the determination of ^{60}Ni . The results indicated that only small amounts of Ca^{2+} and Mg^{2+} were retained on the resin beads, *i.e.*, $\sim 1\%$ at the $1000 \mu\text{g l}^{-1}$ level, and the retained amount remained virtually constant with increased concentration. In order to eliminate the retained part before elution, a wash/pre-elution step was introduced (Step 2 in the operating procedure). This revealed that, by using $120 \mu\text{ l}$ dilute nitric acid

($1:80 \text{ v/v}$) as pre-eluent, no nickel or bismuth was eluted, but the signal of Mg^{2+} diminished to the blank level and that of Ca^{2+} decreased to about 9%. In other words, the majority of the retained alkaline earth metals were eliminated by the pre-elution step, the residual amounts causing no problem for the determination of nickel.

The affinity of the resin for alkali metals is much less than for alkaline earth metals.³³ It is therefore reasonable to conclude that the retention of alkali metals is negligible and, even if some were retained, they were pre-eluted with the alkaline earth metals. The possible residual anions were also eliminated by the pre-elution step.

Performance and validation of the procedure

The characteristic performance data for the procedure are presented in Table 2. Data were obtained by external calibration. Thus, it appears that the enrichment efficiencies for bismuth and nickel were of the same order of magnitude and virtually similar at different uptake flow rates. However, below a concentration of $1.6 \mu\text{g l}^{-1}$ the enrichment efficiency for bismuth changed abruptly to a lower value and remained constant down to $0.04 \mu\text{g l}^{-1}$. This might be related to the preconcentration mechanisms, which presently are unknown. As expected, the detection limits for both metals were lowered by increasing the sample uptake flow rate from $60 \mu\text{ l min}^{-1}$ to $80 \mu\text{ l min}^{-1}$. The comparatively smaller decrease for nickel might be attributed to the relatively high blank signal of this element.

The procedure was validated by the analysis of a certified reference material (CRM 320, River Sediment) and two human urine samples. The recovery tests for the urine samples were made by spiking the original samples with $4.0 \mu\text{g l}^{-1}$ nickel and bismuth before digestion. The digests of urine samples were determined directly. Because the content of iron in the CRM 320 digest exceeds the tolerance limit, it was further diluted by a factor of 10 for the bismuth measurement, and by a factor of 40 for nickel in order to adjust its concentration within the linear range. The results obtained are listed in Table 3. The Ni content determined for the CRM 320 is in very good agreement with that found previously by applying detection by ETAAS.^{22,23} It should be noted that the uncertainty of Ni in the CRM 320 is nearly 6 times that of the certified value, because the determined concentration and the uncertainty were multiplied by the dilution factor of 40. The uncertainty of the final result was thus increased 40-fold.

Acknowledgement

The authors wish to thank Brothers Hartmanns Foundation and P. A. Fiskers Foundation for financial support. J. W. is indebted to the Technical University of Denmark for allocation of a PhD stipend. Thanks are also due to John Madsen and Anders Sølby of the mechanical workshop of this department for conscientious assistance in constructing the DIHEN.

Table 3 The determination of nickel and bismuth in certified reference material (CRM 320) and human urine samples ($n = 4$). The results were obtained at 95% confidence level

Sample	Bismuth				Nickel			
	Indicated/ $\mu\text{g g}^{-1}$	Found/ $\mu\text{g g}^{-1}$	Spiked/ $\mu\text{g l}^{-1}$	Recovery (%)	Indicated/ $\mu\text{g g}^{-1}$	Found/ $\mu\text{g g}^{-1}$	Spiked/ $\mu\text{g l}^{-1}$	Recovery (%)
CRM 320	0.2 ± 0.5^b	0.41 ± 0.04			75.2 ± 1.4	69.4 ± 8.0		
Urine 1 ^a		2.3 ± 0.2	4.0	93.0		4.0 ± 0.5	4.0	105.3
Urine 2 ^a		1.6 ± 0.2	4.0	93.5		5.9 ± 0.7	4.0	94.8

^aIn $\mu\text{g l}^{-1}$. ^bCompare ref. 34.

References

- 1 K. E. Jarvis, A. L. Gray and R. S. Houk, *Handbook of Inductively Coupled Plasma Mass Spectrometry*, Blackie Academic & Professional, 1st edn., 1992.
- 2 S. D. Tanner, *J. Anal. At. Spectrom.*, 1995, **10**, 905.
- 3 H. Uchida and T. Ito, *J. Anal. At. Spectrom.*, 1994, **9**, 1001.
- 4 E. H. Evans and L. Ebdon, *J. Anal. At. Spectrom.*, 1989, **4**, 299.
- 5 Z. Y. Du and R. S. Houk, *J. Anal. At. Spectrom.*, 2000, **15**, 383.
- 6 L. Moens, F. Vanhaecke, J. Riondato and R. Dams, *J. Anal. At. Spectrom.*, 1995, **10**, 569.
- 7 F. Vanhaecke, J. Riondato, L. Moens and R. Dams, *Fresenius' J. Anal. Chem.*, 1996, **355**, 397.
- 8 H. Vanhoe, J. Goossens and L. Moens, *J. Anal. At. Spectrom.*, 1994, **9**, 177.
- 9 K. E. Jarvis, A. L. Gray and E. McCurdy, *J. Anal. At. Spectrom.*, 1989, **4**, 743.
- 10 J. H. Wang, E. H. Hansen and B. Gammelgaard, *Talanta*, 2001, **54**, 117.
- 11 C. Vandecasteele, M. Nagels, H. Vanhoe and R. Dams, *Anal. Chim. Acta*, 1988, **211**, 91.
- 12 J. L. M. de Boer, P. de Joode and R. Ritsema, *J. Anal. At. Spectrom.*, 1998, **13**, 971.
- 13 J. J. Thompson and R. S. Houk, *Appl. Spectrosc.*, 1987, **1**, 801.
- 14 A. R. Date and M. E. Stuart, *J. Anal. At. Spectrom.*, 1988, **3**, 659.
- 15 C. S. Chen and S. J. Jiang, *Spectrochim. Acta, Part B*, 1996, **51**, 1813.
- 16 Y. L. Chen and S. J. Jiang, *J. Anal. At. Spectrom.*, 2000, **15**, 1578.
- 17 P. Becotte-Haigh, J. F. Tyson and E. Denoyer, *J. Anal. At. Spectrom.*, 1998, **13**, 1327.
- 18 K. W. Warnken, D. Tang, G. A. Gill and P. H. Santschi, *Anal. Chim. Acta*, 2000, **423**, 265.
- 19 V. L. Dressler, D. Pozebon and A. J. Curtius, *Spectrochim. Acta, Part B*, 1998, **53**, 1527.
- 20 K. Akatsuka, T. Suzuki, N. Nobuyama, S. Hoshi, K. Haraguchi, K. Nakagawa, T. Ogata and T. Kato, *J. Anal. At. Spectrom.*, 1998, **13**, 271.
- 21 X. P. Yan, R. Kerrich and M. J. Hendry, *J. Anal. At. Spectrom.*, 1999, **14**, 215.
- 22 J. H. Wang and E. H. Hansen, *Anal. Chim. Acta*, 2000, **424**, 223.
- 23 J. H. Wang and E. H. Hansen, *Anal. Chim. Acta*, 2001, **435**, 331.
- 24 J. Ruzicka and L. Scampavia, *Anal. Chem.*, 1999, **71**, 257A.
- 25 H. Liu and A. Montaser, *Anal. Chem.*, 1994, **66**, 3233.
- 26 S. Augagneur, B. Medina, J. Szpunar and R. Lobinski, *J. Anal. At. Spectrom.*, 1996, **11**, 713.
- 27 D. R. Wiederin, F. G. Smith and R. S. Houk, *Anal. Chem.*, 1991, **63**, 219.
- 28 J. A. McLean, H. Zhang and A. Montaser, *Anal. Chem.*, 1998, **70**, 1012.
- 29 M. A. Tarr, G. Zhu and R. F. Browner, *Anal. Chem.*, 1993, **65**, 1689.
- 30 T. W. May and R. H. Wiedmeyer, *At. Spectrosc.*, 1999, **19**(5), 150.
- 31 S. M. Graham and R. V. O. Robert, *Talanta*, 1994, **41**, 1369.
- 32 J. H. Wang and E. H. Hansen, *At. Spectrosc.*, 2001, **22**, 312.
- 33 J. Minczewski, J. Chwastowask and R. Dybczynski, *Separation and preconcentration methods in inorganic trace analysis*, Ellis Horwood, 1982, p. 324.
- 34 E. Ivanova, X. P. Yan and F. Adams, *Anal. Chim. Acta*, 1999, **354**, 7.